

Geochemistry of Sandstones from the Aghajari Formation, Folded Zagros Zone, Southwestern Iran: Implication for Paleoweathering condition, Provenance, and Tectonic Setting

Mohammad Sahraeyan¹ and Mohammad Bahrami²

¹Department of geology, Khorasgan (Esfahan) Branch, Islamic Azad University, Esfahan, Iran

E-mail: M.Sahraeyan@yahoo.com

²Department of geology, Fars Science and Research Branch, Islamic Azad University, Shiraz, Iran

E-mail: Mbahrami1329@yahoo.com

Abstract

The Late Miocene- Pliocene Aghajari Formation is exposed throughout the Folded Zagros Zone and consists of fluvial sediments. Aghajari Formation sandstones are characterized by low to moderate SiO₂ contents, variable abundances of major elements and a relatively high proportion of ferromagnesian elements. Evidence from discrimination diagrams of sedimentary provenance, tectonic setting, major element geochemistry, and Sc/Th, Cr/Th, Co/Th, Zr/ Sc, La/Sc, La/Co, Cr/Sc, and Y/Ni values show that the Aghajari Formation sediments were derived from felsic and intermediate sources. The chemical index of alteration (CIA: 59.2– 77.14) revealed low to moderately weathered source rocks. The major and trace element concentrations indicate deposition in an active continental margin and passive continental margin settings.

Keywords: *Aghajari Formation, Folded Zagros Zone, Sandstone, Geochemistry, Iran.*

1 Introduction

Geochemical signatures of basin clastic sedimentary rocks provide important sources of information [1]. In particular the use of immobile major and trace elements that are thought to be carried in the particulate load have been found to be useful indicators of source terrain, weathering, tectonic, and environmental evolution [2, 3, 4]. Trace elements such as rare earth elements (REEs) are relatively insoluble and as a result, their original compositions are not upset during the sedimentary processes. On a global scale, mudstone/shale chemistry reflects the average composition of the continental crust [5]. Because of the fine grained nature and impermeability, mudrocks retain most of the mineral constituents of the source rocks.

The immobile oxides and elements, such as Al_2O_3 , Fe_2O_3 , TiO_2 , Th, Sc, Co, Zr, and REEs, are particularly useful for provenance interpretations. Being immobile phases in aqueous systems, these elements retain the original source concentration within the shale [2, 6, 7, 8, 9, 10, 11]. The whole rock geochemistry is a useful tool for analyzing a tectonically complex region [1, 6].

2 Geology Setting

The geological evidence suggests that the Zagros region was part of a passive continental margin, which subsequently underwent rifting during the Permo-Triassic and collision during the Late Tertiary [12, 13, 14]. In fact, the Zagros fold-thrust belt lies on the northeastern margin of the Arabian plate and has been divided into NW-SE trending structural zones (imbricated and simply folded belt) parallel to the plate margin separated by major fault zones such as the High Zagros and mountain front faults. In addition to the tectonic divisions parallel to the mountain belt, the belt has also been divided laterally to the Lurestan, Dezful embayment and Fars regions from northwest to southeast [15].

The Aghajari Formation is present throughout the Zagros Basin, but, because of its gradual subsidence during deposition, it is best developed in Dezful Embayment (about 3000 meters) and probably increases in the synclines of this region. The Aghajari Formation was studied in detail and formally defined by James and Wynd [16]. Aghajari Formation in its type section, consists of 2966 meters alternation layers of brown to gray calcareous sandstones and red marls with gypsum interlayers, and red siltstones [17]. Aghajari Formation in Zagros Zone is characterized with two lithofacies groups that each develops in internal Fars and northwestern of Dezful Embayment. The first is mostly continental clastic sediments (i.e. mudstone, sandstone, and conglomerate), but the second one, that spreads in coastal Fars, has a marine characteristics (i.e. marl with gypsum inter-layers). Deposition of the Aghajari Formation took place during the Late Miocene- Pliocene [18], but it doesn't have unity in age and becomes younger from northwestern to south-eastern and from northeastern to

southwestern. In the type section, the lower contact with Mishan Formation is dominantly gradual and sometimes abrupt. The upper contact with Bakhtyari Formation is sometimes gradual and conformable and occasionally abrupt and unconformable. In the study area, the lower contact with Razak Formation and the upper contact with Bakhtyari Formation are gradual [15].

Aghajari Formation is equivalent to Fat'ha and Injana Formations in Iraq, Upper Fars and Lower Fars in Syria and Kuwait, and Kial and Jabal Kibrit Formations in Saudi Arabia [19]. The Aghajari Formation includes Lahbari Clastic Member at its upper part. The above mentioned studies focused primarily on oil producing areas (southwestern of Iran). Sedimentology, sedimentary environment, and morphotectonical evolution of Aghajari and Bakhtyari Formations are thought out by Bahrami [20]. A detailed account of the lithology, sedimentary facies, and sedimentary environments of Aghajari Formation is reported by Bahrami [21] and Sahraeyan et al. [22] as fluvial deposits. According to Sahraeyan and Bahrami [15], these sandstones were distinguished as lithic arenite and sublitharenite.

No detailed studies on the geochemistry of this formation have been carried out. The purpose of the present study is to use a geochemical approach to decipher the paleoweathering condition, provenance, and tectonic setting of the Aghajari Formation sandstones from the Folded Zagros Zone. This is the first study that presents these data of Aghajari Formation sediments.

3 Materials and Methods

Sandstone samples from the siliclastic deposits of the Aghajari Formation (Late Miocene- Pliocene) were studied in the present work. Some 75 sandstone samples were collected.

Fifteen of the samples were analyzed by ICP-MS analysis for the major and trace element geochemistry, and gravimetric method for SiO₂ and volatile components. The ICP-MS analysis was carried out at the Geological Survey of Iran laboratory, Iran.

Where CaO* is the amount of CaO incorporated in the silicate fraction of the rock and the values are in molar proportions to emphasize mineralogical relationship [23]. The highly variable values of CaO in the Aghajari Formation sandstones, ranging between 16.66 to 37.18 wt% in sandstone, are because of the secondary CaCO₃.

Sandstone geochemical data was plotted following the classification schemes of Herron [24] and Pettijohn et al. [25]. Composition of the major element oxides of the sandstone was used for provenance determination applying tectonic discriminatory plots of Bhatia [6] and Roser and Korsch [26]. Alike, ratios of the La/Sc versus Ti/Zr and La/Y versus Sc/Cr of the sandstone on binary plots were used for distinguish the tectonic setting.

4 Sandstone Classification

Major and trace elements analyses of 15 Aghajari Formation sandstones are listed in Table 1. From Table 1, it is apparent that most of the samples are moderate to high in SiO_2 (28.68–59.68%), have moderate Al_2O_3 (2.07–7.43%), and a limit range of K_2O (0.37– 1.64%; averaging 1%). In contrast, they possess low average contents of TiO_2 , MnO , CaO , and Na_2O . Fe_2O_3 and MgO are also low and collectively sum to less than 5%.

Bulk chemical variations of the major elements in the mudstone of the Neogene molasse sequence are plotted on variation diagrams using Al_2O_3 along x-axis and compared with Upper Continental Crust (UCC) and Post-Archaean Australian Shale (PAAS) from Taylor and McLennan [2]. The TiO_2 , Al_2O_3 , Fe_2O_3 , K_2O , and SiO_2 in the sandstone samples of the Aghajari Formation are depleted relative to PAAS and UCC (Figs. 1A, B, C, and D). MnO content is a wide range from lower than UCC to higher than PAAS (Fig. 1E). MgO content of the studied samples is mostly lower than PAAS and UCC, excluding two samples whose MgO is similar to PAAS and UCC, also two samples is higher than PAAS and UCC (Fig. 1F). P_2O_5 and Na_2O is dominantly less than UCC and PAAS, excluding a few samples having content similar to PAAS (Figs. 1G and H).

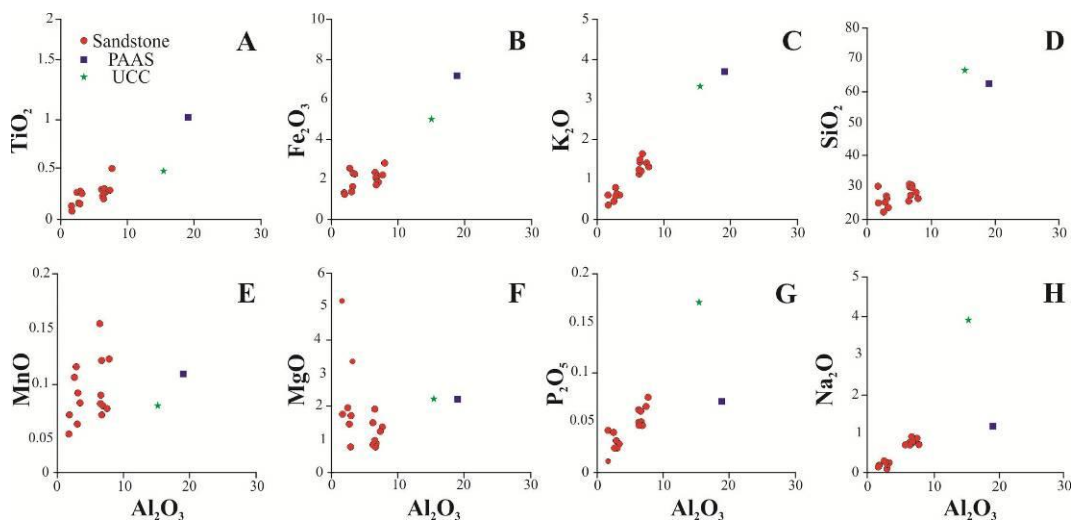


Fig. 2- Various oxides of the sandstone samples of Aghajari Formation plotted against Al_2O_3 . X-axis and Y-axis are weight percent composition. Average data of UCC and PAAS [2] are also plotted for comparison in the binary diagrams.

The less depleted Na_2O contents in the sandstones of the Aghajari Formation compared to the PAAS could be related to the presence of albite and clay minerals. MgO is usually associated with calcite, dolomite, and ferroan carbonates. High MgO levels reflect the presence of carbonate minerals, whereas low concentration

is linked to clay minerals. The depletion of Na₂O compared to PAAS reflect moderate to strong weathering, recycling of the source rock, and their removal during transportation [8, 27, 28].

The high K₂O/Na₂O ratios are attributed to the common presence of K-bearing minerals such as K-feldspar and mica, illite, muscovite, and biotite [29, 30, 31, 32]. A positive correlation between K₂O and Al₂O₃ implies that the concentrations of the K-bearing minerals have significant influence on Al distribution and suggests that the abundance of these elements is primarily controlled by the content of clay minerals [29]. However, a contribution from the feldspars is indicated from their Al₂O₃/SiO₂ ratios. Based on these ratios, the Aghajari Formation sandstones can be classified chemically as lithic arenite, sublitharenite, and Fe-sands [24] (Fig. 2A) and as lithic arenite, subarkose, and sublitharenite [25] (Fig. 2B).

Table 1- Major and trace elements of the selected sandstone samples of the Aghajari Formation sandstones, Folded Zagros Zone, Iran, along with their modified chemical index of alteration (CIA; [23]).

Sample	SiO ₂	TiO ₂	Al ₂ O ₃	Fe ₂ O ₃	MnO	MgO	CaO	Na ₂ O
AJ-5	59.68	0.25	6.28	2.19	0.069	0.85	18.74	0.79
AJ-12	58.17	0.16	2.07	1.46	0.039	5.19	34.98	0.17
AJ-18	57.82	0.28	6.6	1.98	0.067	0.88	18.18	0.82
AJ-26	57.35	0.22	6.32	1.85	0.078	0.9	20.59	0.73
AJ-34	51.07	0.3	7.16	2.34	0.064	1.25	19.74	0.91
AJ-40	58.65	0.27	6.45	2	0.058	0.84	16.66	0.95
AJ-47	41.13	0.3	6.18	2.46	0.151	1.51	28.74	0.7
AJ-56	47.07	0.18	3.19	1.77	0.049	0.77	31.76	0.09
AJ-66	44.1	0.48	7.43	2.91	0.114	1.37	25.7	0.74
AJ-81	28.68	0.28	2.81	2.66	0.096	1.95	37.18	0.3
AJ-87	44.03	0.29	3.25	2.43	0.08	1.73	30.01	0.21
AJ-92	38.94	0.12	2.13	1.44	0.058	1.77	35.99	0.18
AJ-109	47.63	0.3	6.42	2.27	0.113	1.91	26.21	0.78
AJ-116	39.72	0.19	3.03	1.52	0.106	1.46	32.5	0.26
AJ-127	33.68	0.27	3.45	2.38	0.07	3.35	31	0.25

Sample	K ₂ O	P ₂ O ₅	Zr	Nb	Th	Pb	Ga	Zn
AJ-5	1.5	0.048	39.66	8.13	2.98	4.5	8.11	13.01
AJ-12	0.37	0.015	16.72	4.94	0.3	8.41	5.33	0.68
AJ-18	1.64	0.047	38.32	8.9	3.92	0.5	6.82	10.52
AJ-26	1.45	0.016	42.79	7.15	3.8	14.06	7.82	10.76

AJ-34	1.41	0.063	44.18	9.42	6.43	4.69	6.03	15.86
AJ-40	1.22	0.048	34.46	8.65	1.97	4.05	5.31	8.6
AJ-47	1.14	0.06	49	9.84	3.28	13.52	12.96	18.4
AJ-56	0.6	0.027	34.47	5.77	2.96	3.41	4.47	7.19
AJ-66	1.32	0.07	51.77	15.66	6.85	1.01	7.55	19.65
AJ-81	0.46	0.04	31.48	8.44	4	16.04	4.48	12.44
AJ-87	0.64	0.032	34.89	9.35	3.01	5.06	4.92	11.27
AJ-92	0.62	0.042	20.91	3.5	2.41	12.17	7.62	0.62
AJ-109	1.21	0.058	40.7	9.73	4.91	10.73	11.98	18.75
AJ-116	0.8	0.026	24.71	5.84	0.3	18.29	4.13	2.18
AJ-127	0.62	0.03	32.15	8.33	3.83	5.16	5.37	9.6

Sample	Sc	Ta	Co	Li	Be	B	U	W
AJ-5	5.6	0.5	11.12	0.3	0.54	12.12	2.63	1.47
AJ-12	5.11	1.83	0.83	0.3	0.16	10.08	2.45	1.95
AJ-18	5.51	0.77	8.47	0.3	0.52	10.53	3.43	1.19
AJ-26	5.89	0.1	9.3	0.3	0.51	6.44	2.51	1.29
AJ-34	6.79	0.27	15.43	2.48	0.6	16.12	3.63	1.31
AJ-40	6.15	0.15	11.46	0.3	0.56	16.04	2.34	1.28
AJ-47	7.1	0.1	17.42	1.03	0.53	12.51	3.49	1.4
AJ-56	5.22	0.74	11.14	0.3	0.31	10.85	2.62	1.18
AJ-66	8.51	0.29	16.69	1.93	0.58	9.17	4.11	1.59
AJ-81	6.4	0.22	23.39	0.3	0.35	19.99	4.07	1.58
AJ-87	6.17	0.18	17.83	0.3	0.34	7.48	3.27	1.37
AJ-92	3.6	0.4	8.95	0.3	0.24	11.53	2.31	1.64
AJ-109	7.35	0.9	15.27	1.59	0.53	5.51	3.17	1.56
AJ-116	4.46	0.67	10.92	0.3	0.3	8.74	2.79	1.28
AJ-127	6.99	0.1	24.7	0.3	0.29	9.24	3.28	1.78

Sample	Pr	Nd	Sm	Eu	Gd	Y	Mo	Ni
AJ-5	1.69	6.24	2.43	0.71	1.72	10.01	21.24	50.61
AJ-12	1.37	0.14	1.92	0.37	0.75	5.32	10.67	92.7
AJ-18	1.77	8.81	2.2	0.66	1.78	9.86	12.04	34.16
AJ-26	1.9	7.3	2.35	0.54	1.66	10.18	10.05	39.64
AJ-34	1.68	7.89	2.98	0.63	1.55	10.2	13.33	68.72
AJ-40	1.76	8.68	3.26	0.77	1.68	9.33	19.39	42.26
AJ-47	2.12	6.48	2.75	0.64	1.91	12.3	8.54	82.38
AJ-56	1.69	6.6	1.35	0.59	1.28	9.51	11.36	71.87

AJ-66	2.66	13.54	3.51	0.95	2.44	14.77	17.25	60.11
AJ-81	2.52	4.91	2.46	0.57	1.6	8.82	10.4	134
AJ-87	2.57	2.22	3.12	0.67	1.49	9.73	11.86	106
AJ-92	1.79	3.88	1.94	0.38	1.14	6.79	22.49	47.11
AJ-109	1.71	9.94	2.36	0.82	1.65	12.64	14.95	91.12
AJ-116	1.85	4.04	2.55	0.54	1.19	8.15	11.3	47.37
AJ-127	2.71	2.6	2.5	0.47	1.39	8.4	10.62	153

Sample	Ba	Rb	Sr	Ho	Hf	Cs	La	Ce
AJ-5	297	150	212	0.74	6.09	3.12	16.83	25.65
AJ-12	45	132	211	0.7	1.24	3.43	6.15	0.75
AJ-18	220	146	212	0.59	7.63	2.29	15.22	18.99
AJ-26	189	148	197	0.68	7.29	2.21	15.81	17.79
AJ-34	245	146	222	0.75	3.83	3.09	15.77	19.25
AJ-40	267	150	180	0.65	2.8	2.78	16.36	17.78
AJ-47	519	152	346	0.77	4.34	3.44	17.22	19.88
AJ-56	68	136	183	0.73	1.24	2.75	10.66	6.65
AJ-66	192	126	288	0.94	4.82	3.71	23.54	31.15
AJ-81	104	124	377	0.87	5.5	4.55	11.54	6.63
AJ-87	112	120	277	0.78	3.48	3.76	12.63	13.47
AJ-92	398	128	256	0.65	3.05	2.93	9.16	2.22
AJ-109	218	137	436	0.79	1.66	3.32	18.01	21.98
AJ-116	185	126	382	0.59	3.61	2.82	11.6	11.6
AJ-127	537	141	247	0.67	0.04	3.98	10	8.82

Sample	Dy	Er	Tm	Yb	Sn	V	Cu	CIA
AJ-5	1.18	0.51	1.38	0.9	0.68	60.49	58.15	59.79
AJ-12	0.7	0.5	0.97	0.68	0.5	60.19	22.59	68.32
AJ-18	0.91	0.55	1.13	0.91	0.61	57.76	25.68	59.6
AJ-26	1.14	0.5	1.22	0.89	0.56	49.05	17.1	61.41
AJ-34	0.96	0.58	0.94	0.94	0.76	61.73	19.19	61.3
AJ-40	0.61	0.53	1.12	0.88	0.63	52.45	20.26	59.2
AJ-47	1.08	0.61	1.27	1.15	0.74	64.21	19.12	63.6
AJ-56	1.26	0.5	1.25	0.89	0.53	48	16.33	77.14
AJ-66	1.32	0.96	1.6	1.38	0.95	97.05	15.18	65.79
AJ-81	0.39	0.53	1.36	0.95	0.89	78.58	29.48	65.43
AJ-87	1.3	0.59	1.46	0.94	0.74	91.01	29.02	70.14
AJ-92	0.72	0.5	1.13	0.65	0.45	46.94	12.06	62.77

AJ-109	1.4	0.6	1.45	1.09	0.72	60.06	17.36	62.35
AJ-116	0.91	0.5	1.09	0.88	0.54	57.74	13.53	63.77
AJ-127	0.73	0.52	1.38	0.88	0.75	79.51	14.31	69.79

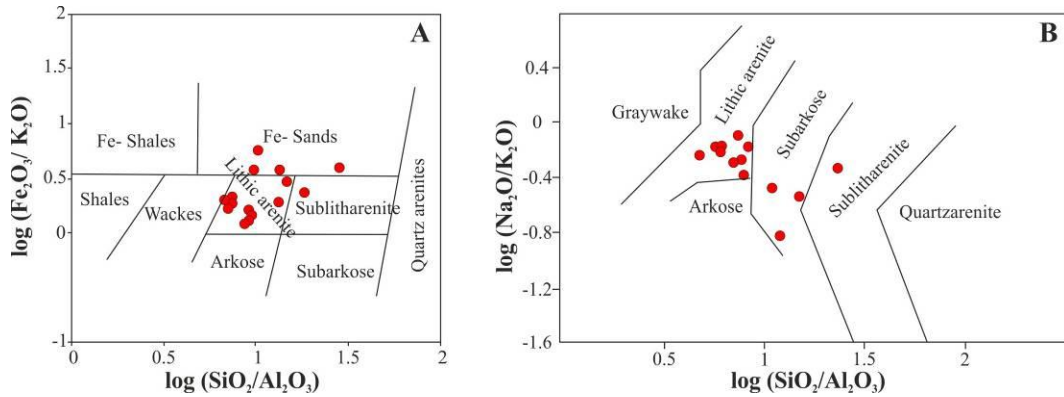


Fig. 2- Chemical classification of samples from the Aghajari Formation sandstones based on binary diagrams. A: $\log(\text{SiO}_2/\text{Al}_2\text{O}_3)$ versus $\log(\text{Fe}_2\text{O}_3/\text{K}_2\text{O})$ diagram of Herron ^[24]; B: the $\log(\text{SiO}_2/\text{Al}_2\text{O}_3)$ versus $\log(\text{Na}_2\text{O}/\text{K}_2\text{O})$ diagram of Pettijohn et al. ^[25].

5 Provenance

The concentration of Zr is used for characterizing the nature and composition of source rocks [9, 11]. The high TiO_2/Zr ratios (52.3–96.9) of the sandstones indicate intermediate source rocks [2, 4, 8, 33, 34]. When plotted on the TiO_2 -Zr diagrams (Fig. 3), these ratios help distinguish among three different source rock types, i.e., felsic, intermediate, and mafic. The TiO_2 versus Zr plot of the sandstones represents predominately intermediate source rocks.

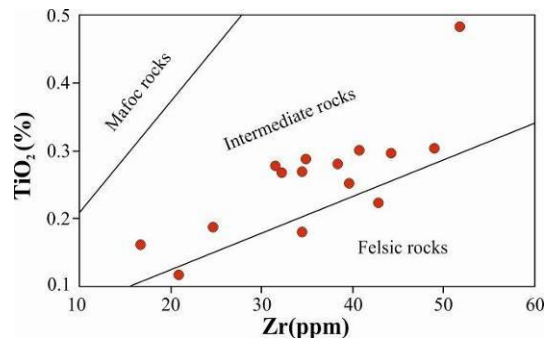


Fig. 3- TiO_2 -Zr plot for the Aghajari Formation sandstones (after [9]).

Trace elements such as Cr, Ni, Co, and V are useful indicators of mafic and ultramafic sources [28, 33]. Felsic source rocks usually contain lower concentrations of Cr, Co, Ni, and V and higher concentrations of Ba, Sr, Y, and Zr than mafic and intermediate source rocks [2, 28, 34]. The respective average values of the sandstone samples (Cr= 220, Ni= 74.73, Co= 13.52, and V= 64.32) are similar/or higher than those in the upper continental crust and PAAS [2].

In the discrimination diagrams for sedimentary provenance after Roser and Korsch [26], all samples of the studied sandstones plot in the quartzose recycled field (Fig. 4).

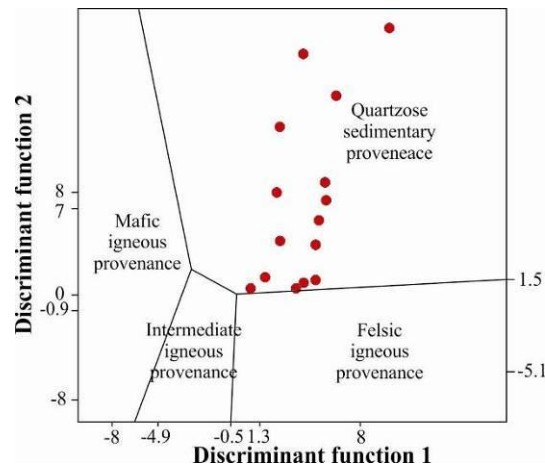


Fig. 4- Provenance discriminant function diagram using major elements for Aghajari Formation sandstones (after [26]).

The variations in Th and La (indicative of felsic) and, Sc and Co (indicative of mafic) contents have been used to differentiate between felsic and mafic provenance by various authors [10, 35, 36, 37, 38]. Th/Co versus La/Sc bivariate diagram can provide information regarding the source rock characteristics [36, 39]. The Th/Co versus La/Sc plot (Fig. 5) suggests a silicic nature of the source rocks [36].

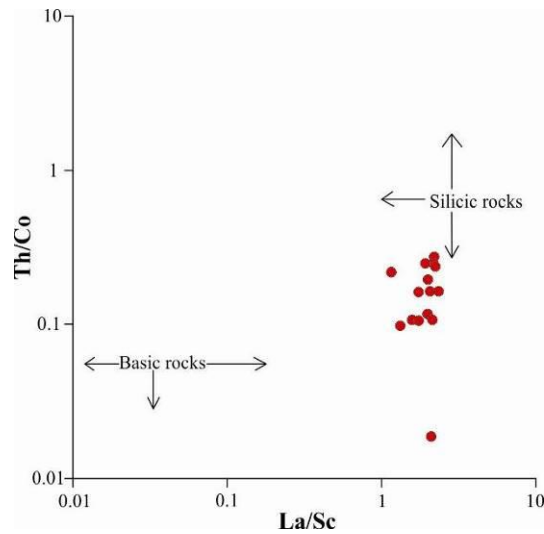


Fig. 5- Th/Co vs. La/Sc plot showing source rock composition for the Aghajari Formation sandstones (after ^[36]).

6 Tectonic Setting

The major element geochemistry of sandstones can be used for drawing inferences related to the provenance type and the plate tectonic setting of ancient sedimentary basins [6, 26, 40].

The geochemical data obtained are consistent with those of Aghajari Formation sandstones, deposited in an active and passive margin settings [6]. The optimum discrimination of sandstones representing the various tectonic settings is achieved by the plots of $\text{Fe}_2\text{O}_3 + \text{MgO}$ versus TiO_2 , $\text{Al}_2\text{O}_3 / \text{SiO}_2$, $\text{K}_2\text{O} / \text{Na}_2\text{O}$, and $\text{Al}_2\text{O}_3 / (\text{CaO} + \text{Na}_2\text{O})$ (Fig. 6). Active continental margin sandstones are dominantly derived from the uplifted basement and reflect the composition of the upper continental crust [6]. Sediments of passive continental margins generally are considered to be mature [41, 42], and are deposited in plate interiors at stable continental margin or intra-cratonic basins. The Aghajari Formation sandstones are plotted in the field of the active and passive continental margin settings.

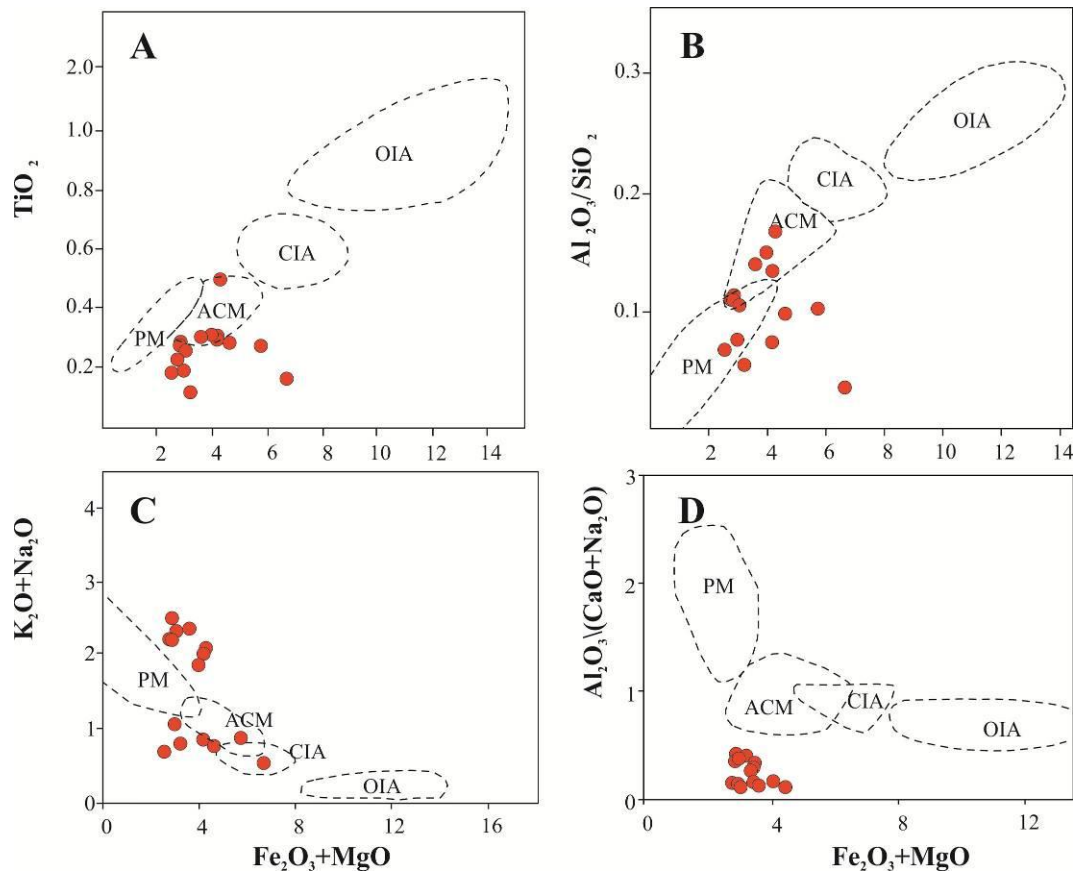


Fig. 6- Plots of the major element composition of the Aghajari Formation sandstones on the tectonic setting discrimination diagrams of Bhatia [6]. OIA: Oceanic island Arc, CIA: continental island Arc, ACM: active continental margin, PM: passive continental margin.

The K_2O / Na_2O versus SiO_2 diagram is widely used for discriminating between sediments deposited in the passive margin, active margin, and island arc settings [26]. The ratio of K_2O / Na_2O variation with SiO_2 is plotted in a binary diagram to understand the tectonic setting of the Aghajari Formation sediments (Fig. 7A). It is found from this plot that all samples are plotted in the active and passive continental margin fields. The same pattern is observed when the sandstone samples are plotted on the SiO_2 / Al_2O_3 versus $Na_2O + K_2O$ diagram (Fig. 7B).

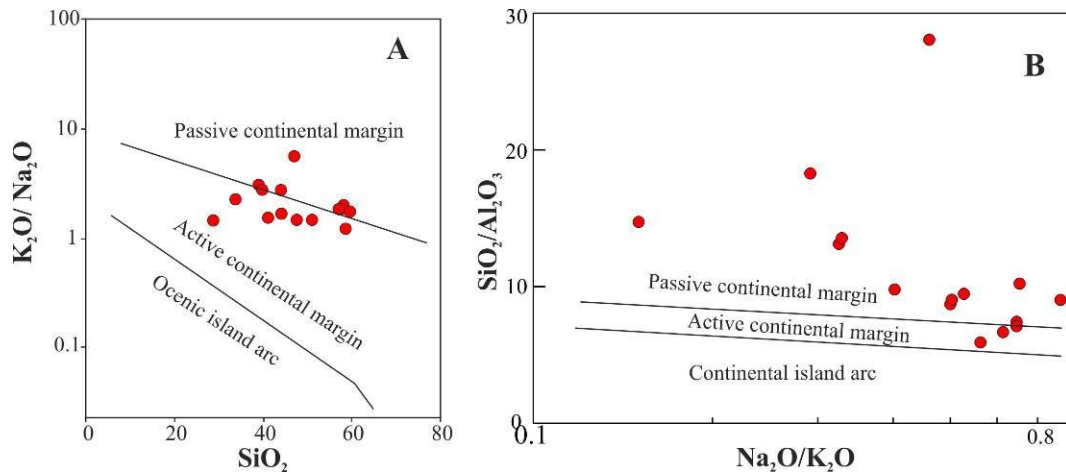


Fig. 7- Tectonic setting discrimination diagrams based on major element compositions of Aghajari Formation sandstone samples. A: K_2O/Na_2O versus SiO_2 ; B: SiO_2/Al_2O_3 versus K_2O/Na_2O (after [26]).

Also, plotting chemical contents of the studied sediments on the discrimination diagram of Bhatia [6] (Fig. 8) indicate that the samples fall within the active and passive margin fields.

Trace elements (e.g., Ti, Co, La, Th, Sc, and Zr) in the clastic sedimentary rocks are considered to be immobile under conditions of weathering, diagenesis, and moderate levels of metamorphism, and are commonly preserved in sedimentary rocks. Therefore, the trace elements represent well-established provenance and tectonic setting indicators [26, 34, 44]. On the Th-Sc-Zr/10 diagram (Fig. 9A), data related to the sandstone samples are plotted in the active continental margin setting; one of the data elements is plotted in continental island arc setting and one is plotted outside the settings. When plotted on the La/Sc versus Ti/Zr and La/Y versus Sc/Cr discrimination diagrams of Bhatia and Crook^[26] (Figs. 9B and C), most of sandstone samples cluster within the active continental margin and passive continental margin fields, respectively.

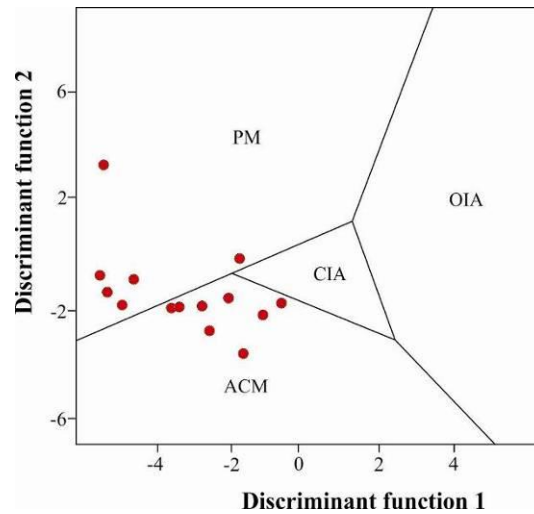


Fig. 8- Plots of the major element composition of the Aghajari Formation sandstones on the tectonic setting discrimination diagrams of Bhatia ^[6]. OIA: Oceanic island Arc; CIA: Continental island Arc; ACM: Active continental margin; PM: Passive continental margin.

7 Source Area Weathering

Chemical weathering affects, to a great extent, the composition of siliciclastic sediments. Through these processes the large cations (e.g. Ba, Al) remain preserved in the weathering residue in contrast to the smaller cations (Na, Ca, Sr) that can be selectively removed [30, 45].

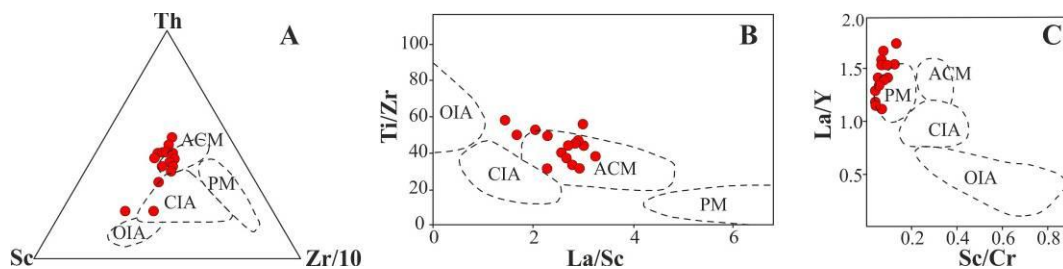


Fig. 9- Plots of the trace element composition of the Aghajari Formation sandstone samples on the tectonic setting discrimination diagrams of Bhatia and Crook [26]. OIA: Oceanic island Arc; CIA: Continental island Arc; ACM: Active continental margin; PM: Passive continental margin.

The degree of weathering may be assessed by the Chemical index of alteration (CIA = $100 \times [Al_2O_3 / (Al_2O_3 + CaO^* + Na_2O + K_2O)]$; ^[23]). All data in this formula is molecular proportions. CaO^* represents the value of Ca in the silicate fraction only. No carbonates were found in the samples examined. According to

the methods of McLennan [46], we calculated and corrected CaO^* . CaO corrected for apatite using P_2O_5 ($\text{CaO}^* = \text{CaO} - (10/3 \times \text{P}_2\text{O}_5)$). If the corrected CaO^* was less than the amount of Na_2O , this corrected CaO^* value was adopted. In this regard, if the CaO^* value is greater than the amount of Na_2O , it was assumed that the concentration of CaO equals that of Na_2O .

The CIA values of approximately 50 imply an unweathered upper crust or weak weathering, whereas CIA values of 100 indicate intense weathering with a complete removal of alkali and alkaline earth elements and an increase in Al_2O_3 [46, 47, 48]. The calculated CIA values (Table 1) of sandstone samples range from 59.2 to 77.14, with an average of 64.69. However, most samples have values greater than 60, suggesting moderate to high weathering either of the original source or during transport before deposition. Its lower part show lower alteration values (CIA) than the upper part.

8 Conclusion

Element composition, inter-element ratios (e.g., $\text{Na}_2\text{O}/\text{K}_2\text{O}$, $\text{Al}_2\text{O}_3/\text{TiO}_2$, TiO_2/Zr , K/Rb , La/Co , Cr/Ni , Co/Th , La/Sc , Sc/Th , Cr/Th , Y/Ni , Cr/Zr , and Zr/Sc), and source rock discrimination diagrams (e.g., SiO_2 versus $\text{K}_2\text{O} / \text{Na}_2\text{O}$, $\text{SiO}_2/\text{Al}_2\text{O}_3$ versus $\text{K}_2\text{O}/\text{Na}_2\text{O}$, $\text{Al}_2\text{O}_3/\text{SiO}_2$ versus $\text{Fe}_2\text{O}_3 + \text{MgO}$, $\text{Al}_2\text{O}_3/(\text{CaO} + \text{Na}_2\text{O})$ versus $\text{Fe}_2\text{O}_3 + \text{MgO}$, TiO_2 versus $\text{Fe}_2\text{O}_3 + \text{MgO}$, $\text{K}_2\text{O}/\text{Na}_2\text{O}$ versus $\text{Fe}_2\text{O}_3 + \text{MgO}$, $\text{Th}-\text{Sc}-\text{Zr}/10$, Ti/Zr versus La/Sc , and La/Y versus Sc/Cr), indicate that the Aghajari Formation sediments originated from felsic and intermediate, moderate weathering source rocks within the active and passive continental margin settings. The low/moderate CIA values as well as the low Th/Sc ratio^[4] suggest that the source rocks for the Aghajari Formation sediments might be from a mixed old continental source, composed of granitic plutonic rocks. Sandstone samples with a high abundance of Cr and a high ratio of Th/Sc were most likely to be derived from a mafic provenance. Moreover, the obtained data are consistent with a long distance transport, in a variable climate, over the Arabian shield, which supplied these sands to their depositional basin along the passive margin of the Late Miocene-Pliocene Zagros foreland basin.

Acknowledgements

We thank the Islamic Azad University, Khorasgan (Esfahan) Branch and Geological Survey of Iran for providing laboratory equipments. In addition, we are grateful to Dr S.H. Hejazi, A. Heydari, H. Heydari, M. Farajzadeh and J. Maniani for their considerable help throughout this study.

References

- [1] Yan, Y., Xia, B., Lin, G., et al., "Geochemistry of the sedimentary rocks from the Nanxiong Basin, South China and implications for provenance, paleoenvironment and paleoclimate at the K/T boundary", *Sedimentary Geology*, Vol. 197, (2007), pp. 127-140.
- [2] Taylor, S.R., McLennan, S.M., *The continental crust: Its composition and evolution*, Blackwell Scientific, Oxford, (1985).
- [3] Roser, B.P., Korsch, R.J., "Provenance signatures of sandstone- mudstone suites determined using discriminant function analysis of major-element data", *Chemical Geology*, Vol. 67, (1988), pp. 119- 139.
- [4] Cullers, R.L., "The geochemistry of shales, siltstones and sandstones of Pennsylvanian-Permian age, Colorado, USA: Implications for provenance and metamorphic studies", *Lithos*, Vol. 51, (2000), pp. 181- 203.
- [5] Qiugen, L., Shuwen, L., Baofu, H., et al., "Geochemical characteristics of the metapelites from the Xingxingxia group in the eastern segments of the Central Tianshan: Implications for the provenance and paleoweathering", *Science in China Series D Earth Sciences*, Vol. 48, (2005), pp. 1637- 1648.
- [6] Bhatia, M.R., "Plate tectonics and geochemical composition of sandstones", *Journal of Geology*, Vol. 92, (1983), pp. 181- 193.
- [7] Blatt, H., "Provenance studies and mudrocks", *Journal of Sedimentary Petrology*, Vol. 55, (1985), pp. 69- 75.
- [8] Condie, K.C., "Chemical composition and evolution of upper continental crust: contrasting results from surface samples and shales", *Chemical Geology*, Vol. 104, (1993), pp. 1- 37.
- [9] Hayashi, K., Fujisawa, H., Holland, H.D., et al., "Geochemistry of 1.9 Ga sedimentary rocks from northeastern Labrador, Canada", *Geochimica et Cosmochimica Acta*, Vol. 61, (1997), pp. 4115- 4137.
- [10] Kasanzu, C., Maboko, M.A.H., Manya, S., "Geochemisrty of fine grained clastic sedimentary rocks of the Neoproterozoic Ikorongo Group, NE Tanzania: Implication for provenance and source rock weathering", *Precambrian Research*, Vol. 164, (2008), pp. 201- 213.
- [11] Paikaray, S., Banerjee, S., Mukherji, S., "Geochemistry of shales from Paleoproterozoic to Neoproterozoic Vindhyan Supergroup: Implicayions on provenance, tectonics and paleoweathering", *Journal of Asian Earth Sciences*, Vol. 32, (2008), pp. 34- 48.
- [12] Stocklin, J., Possible ancient continental margins in Iran, In: Burk, C.A., Drake, C.L. (Eds), *The Geology of Continental Margins*. New York, Springer, 1974, pp. 873- 887.
- [13] Berberian, M., King, G.C.P., "Towards the paleogeography and tectonic evolution of Iran", *Canadian Journal of the Earth Sciences*, Vol. 18, (1981), pp. 210- 265.

- [14] Beydoun, Z.R., Hughes Clarke, M.W., Stoneley, R., "Petroleum in the Zagros basin: A Late Tertiary foreland basin overprinted onto the outer edge of a vast hydrocarbon- rich Palaeozoic– Mesozoic passive margin shelf", *AAPG Bulletin*, Vol. 55, (1992), pp. 309- 339.
- [15] Sahraeyan, M., Bahrami, M., " Petrography and provenance of sandstones from the Aghajari Formation, Folded Zagros Zone, southwestern Iran", *International Journal of Basic and Applied Sciences*, Vol. 1, No. 3, (2012), pp. 283- 298.
- [16] James, G.A., Wynd, J.G., "Stratigraphic nomenclature of Iranian oil consortium agreement Area", *AAPG Bulletin*, Vol. 49, No. 12, (1965), pp. 2182- 2245.
- [17] Motiei, H., *Stratigraphy of Zagros*, Tehran, Geological Survey of Iran, (1993).
- [18] Stocklin, J., *Stratigraphic Lexicon of Iran*, Geological Survey Of Iran, Report No. 18, 1977.
- [19] Al-Husseini, M.I., "Middle East Geological Timescale 2008", *Journal of Middle East Petroleum and Geoscience*, Vol. 13, No. 4, (2008).
- [20] Bahrami, M., "Sedimentology and morphotectonical evolution of Aghajari and Bakhtiari Formations in north-western of Shiraz, Iran", *Journal of Science, Islamic Azad University*, Vol. 8, No. 27&28, (1998), pp. 1995- 2010.
- [21] Bahrami, M., "Lithofacies and Sedimentary Environments of Aghajari Formation in Dehsheikh Mountain, West of Shiraz, Iran", *World Applied Science Journal*, Vol. 6, No. 4, (2009), pp. 464- 473.
- [22] Sahraeyan, M., Bahrami, M., Hejazi, S.H., "Facies and sedimentary environments of Aghajari Formation in southeast of Sarvestan, Folded Zagros Zone, Iran", *Proceedings of the conference of application of earth sciences in fundamental researchs of Iran*, (2011), pp. 168- 175.
- [23] Nesbitt, H.W., Young, G.M., "Early Proterozoic climates and plate motions inferred from major element chemistry of lutites", *Nature*, Vol. 299, (1982), pp. 715- 717.
- [24] Herron, M.M., "Geochemical classification of terrigenous sands and shales from core or log data", *Journal of Sedimentary Petrology*, Vol. 58, (1988), pp. 820- 829.
- [25] Pettijohn, F.J., Potter, P.E., Siever, R., *Sand and Sandstone*, second ed., Springer, New York, (1987).
- [26] Roser, B.P., Korsch, R.J., "Determination of tectonic setting of sandstone mudstone suites using SiO₂ content and K₂O/Na₂O ratio", *Journal of Geology*, Vol. 94, (1986), pp. 635- 650.
- [27] Nesbitt, H.W., Markovics, G., Price, R.C., "Chemical processes affecting alkalis and alkaline earths during continental weathering", *Geochimica et Cosmochimica Acta*, Vol. 44, (1980), pp. 1659- 1666.
- [28] Wronkiewicz, D.J., Condie, K.C., "Geochemistry of Archean shales from the Witwatersland Supergroup, South Africa: source area weathering and provenance", *Geochimica et Cosmochimica Acta*, Vol. 51, (1987), pp. 2401- 2416.

- [29] McLennan, S.M., Taylor, S.R., Eriksson, K.A., "Geochemistry of Archaean shales from the Pilbara Supergroup, Western Australia", *Geochimica et Cosmochimica Acta*, Vol. 47, No. 7, (1983), pp. 1211- 1222.
- [30] Nath, B.N., Kunzendorf, H., Pluger, W.L., "Influence of provenance, weathering and sedimentary processes on the elemental ratio of the fine-grained fraction of the bed load sediments from the Vembanad Lake and the adjoining continental shelf, southwest Coast of India", *Journal of Sedimentary Research*, Vol. 70, (2000), pp. 1081- 1094.
- [31] Zhang, K.L., "Secular geochemical variations of the Lower Cretaceous siliciclastic from central Tibet (China) indicate a tectonic transition from continental collision to back-arc rifting", *Earth and Planetary Science Letters*, Vol. 229, (2004), pp. 73- 89.
- [32] Osaе, S., Asiedu, D.K., Yakubo, B., et al., "Provenance and tectonic setting of Late Proterozoic Buem sandstones of southeastern Ghana: Evidence from geochemistry and detrital modes", *Journal of African Earth Science*, Vol. 44, (2006), pp. 85- 96.
- [33] Huntsman-Mapila, P., Kampunzu, A.B., Vink, B., et al., "Cryptic indicators of provenance from the geochemistry of the Okavango Delta sediments, Bostwana", *Sedimentary Geology*, Vol. 174, (2005), pp. 123- 148.
- [34] Spalletti, L.A., Queralt, I., Matheos, S.D., et al., "Sedimentary petrology and geochemistry of siliciclastic rocks from the upper Jurassic Tordillo Formation (Neuquen Basin, western Argentina): Implications for provenance and tectonic setting", *Journal of South American Earth Sciences*, Vol. 25, (2008), pp. 440- 463.
- [35] McLennan, S.M., Nance, W.B., Taylor, S.R., "Rare earth element-thorium correlations in sedimentary rocks and the composition of the continental crust", *Geochimica et Cosmochimica Acta*, Vol. 44, (1980), pp. 1833- 1839.
- [36] Cullers, R.L., "Implications of elemental concentrations for provenance, redox conditions, and metamorphic studies of shales and limestones near Pueblo, CO, USA", *Chemical Geology*, Vol. 191, No. 4, (2002), pp. 305- 327.
- [37] Nagarajan, R., Armstrong-Altrin, J.S., Nagendra, R., et al., "Petrography and geochemistry of terrigenous sedimentary rocks in the Neoproterozoic Rabanpalli Formation, Bhima Basin, southern India: Implications for paleoweathering condition, provenance, and source rock composition", *Journal of Geology Society of India*, Vol. 70, No. 2, (2007a), pp. 297- 312.
- [38] Nagarajan, R., Madhavaraju, J., Nagendra, R., et al., "Geochemistry of Neoproterozoic shales of Rabanpalli Formation, Bhima Basin, Northern Karnataka, Southern India: Implications for provenance and paleoredox conditions", *Revista Mexicana Ciencias Geologicas*, Vol. 24, No. 2, (2007b), pp. 150- 160.
- [39] McLennan, S.M., Taylor, S.R., "Sedimentary rocks and crustal evolution: tectonic setting and secular trends", *Journal of Geology*, Vol. 99, (1991), pp. 1- 21.

- [40] Armstrong-Altrin, J.S., Lee, Y., Verma, S., et al., "Geochemistry of sandstones from the Upper Miocene Kudanul Formation, southern India: Implications for provenance, weathering tectonic setting", *Journal of Sedimentary Research*, Vol. 74, (2004), pp. 167- 179.
- [41] Crook, K.A.W., Lithogenesis and tectonics: the significance of compositional variation in flysch arenites (greywackes), In: Dott, R.H., Shaver, R.H. (Eds), *Modern and Ancient Geosynclinal Sedimentation*, Special Publication 19, Society of Economic Geologists and Paleontologists, 1974, 304- 310.
- [42] Schwab, F.L., "Framework mineralogy and chemical composition of continental margin-type sandstone", *Geology*, Vol. 3, (1975), pp. 487- 490.
- [43] Bhatia, M.R., Crook, K.A.W., "Trace element characteristics of graywackes and tectonic setting discrimination of sedimentary basins", *Contributions to Mineralogy and Petrology*, Vol. 92, (1986), pp. 181- 193.
- [44] McLennan, S.M., Hemming, S., McDaniel, D.K., et al., Geochemical approaches to sedimentation, provenance, and tectonics. In: Johnsson, M.J., Basu, A. (Eds), *Processes controlling the composition of clastic sediments*, *Geology Society of American Special Paper*, Vol. 284, (1993), pp. 21- 40.
- [45] Fedo, C.M., Eriksson, K., Krogstad, E.J., "Geochemistry of shales from the Archean (3.0 Ga.) Buhwa Greenstone Belt, Zimbabwe: Implications for provenance and source area weathering", *Geochimica et Cosmochimica Acta*, Vol. 60, (1996), pp. 1751- 1763.
- [46] McLennan, S.M., "Weathering and global denudation", *Journal of Geology*, Vol. 101, (1993), pp. 295- 303.
- [47] Fedo, C.M., Nesbitt, H.W., Young, G.M., "Unraveling the effects of potassium metasomatism in sedimentary rock sand paleosols, with implications for paleoweathering conditions and provenance", *Geology*, Vol. 23, (1995), pp. 921- 924.
- [48] Dupuis, C., Hebert, R., Cote, V.D., et al., "Geochemistry of sedimentary rocks melange and flysch units south of the Yarlung Zangbo suture zone, southern Tibet", *Journal of Asian Earth Sciences*, Vol. 26, (2006), pp. 489- 508.